OPEN ACCESS Int. J. Phytopathol. 15 (01) 2026. 87-96 DOI: 10.33687/phytopath.015.01.6102

Check for updates

Available Online at EScience Press

International Journal of Phytopathology

ISSN: 2312-9344 (Online), 2313-1241 (Print)

https://esciencepress.net/journals/phytopath

ECOLOGICAL NICHE PARTITIONING OF *SCLEROTIUM ROLFSII* AND *RALSTONIA SOLANACEARUM* IN TOMATO AGROECOSYSTEMS IN CÔTE D'IVOIRE

[a,b]YASSOGUI Koné*, [B]AMARI L. D. G. Elisée, [c]AFFERY A. Martin, [c]PAKORA G. Alex

[a] *Université Félix Houphouët-Boigny, UFR Biosciences, UPR Physiologie et Pathologie Végétale, 22 BP 582, Abidjan 22, Côte d'Ivoire.*

[b] *WASCAL / African Center of Excellence in Climate Change, Biodiversity and Sustainable Agriculture, Pôle Scientifique et d'Innovation, Bingerville, Université Félix Houphouët-Boigny (UFHB), 01 BP V 34, Abidjan 01, Côte d'Ivoire.*

[c] *Université de MAN, UFR Ingénierie Agronomique, Forestière et Environnementale (UFR-IAFE), BP 20 Man, Côte d'Ivoire.*

ARTICLEINFO

Article History
Received: February 19, 2026
Revised: April 23, 2026
Accepted: April 29, 2026

Keywords
Bacterial wilt
Southern blight
Soilborne pathogens
Edaphic factors
Landscape epidemiology

ABSTRACT

A cross-sectional survey was conducted across 150 tomato (*Solanum lycopersicum* L.) plots in five agroecological zones in Côte d'Ivoire to test the hypothesis of ecological niche partitioning between *Sclerotium rolfsii* Sacc. and *Ralstonia solanacearum* (Smith). Co-occurrence analysis using a Chi-square test revealed statistical independence between the pathogens (Odds Ratio = 1.18; p = 0.834), rejecting the synergy hypothesis. The observed spatial segregation is consistent with environmental filtering as a structuring process. *R. solanacearum* formed an endemic hotspot in the humid coastal zone, significantly associated with acidic soils (Spearman's ρ = −0.28; p < 0.001) and hydromorphic lowlands. Conversely, *S. rolfsii* exhibited a greater disease intensity/severity (DSI) in savanna zones, showing a significant positive correlation with organic matter (ρ = + 0.23; p < 0.01). These results suggest that this soilborne pathogen community is associated with divergent ecological optima rather than direct competition. This advocates for spatially differentiated management based on local edaphic risk factors, paving the way for precision crop protection in tropical agroecosystems.

Corresponding Author: YASSOGUI Koné

Email: yasskone2016@gmail.com +225 0554326622/ +225 0709476568

INTRODUCTION

In sub-Saharan Africa, tomato (*Solanum lycopersicum* L.) constitutes a cornerstone of food security and the agricultural economy. However, this crop is severely constrained by soilborne biotic pressure, responsible for yield losses ranging from 30% to 100% depending on production basins (Wang *et al.,* 2023). In Côte d'Ivoire, the sustainability of vegetable farming systems is threatened by the persistence of two major agents: the fungus *Sclerotium rolfsii* Sacc. responsible for up to 41% of tomato yield losses in humid forest zones (Bolou *et al*., 2016), and the bacterium *Ralstonia solanacearum* (Smith). The ability of these pathogens to survive durably as sclerotia or in viable but non-culturable (VBNC) states transforms infested soils into complex epidemiological reservoirs, often rendering conventional control methods ineffective (Liu *et al.,* 2023).

Historically, plant pathology has addressed these constraints through the classical approach of the disease triangle. While the recent concept of the pathobiome has enabled a better understanding of the complexity of interactions among microorganisms, it often tends to presuppose synergistic dynamics between sympatric agents (Lamichhane & Venturi, 2015). This perspective, however, risks obscuring the community assembly mechanisms governed by ecological niche theory.

Recent work suggests that the distribution of soilborne pathogens is primarily governed by environmental filtering, where species are sorted by precise physicochemical gradients (Wei *et al.,* 2019; Liu *et al.,* 2023). This theoretical framework posits that local abiotic conditions act as sieves selecting species whose functional traits are compatible with the environment (Fodor, 2011). Although the individual preferences of *R. solanacearum* for acidic soils (Caldwell *et al*., 2017) and of *S. rolfsii* for organic residues are documented, no study has, to date, quantified the spatial segregation of this soilborne pathogen community at the scale of a tropical latitudinal gradient.

Recent epidemiological surveys in neighbouring West African agroecosystems provide relevant regional context. Dossoumou *et al*. (2023) reported *R. solanacearum* prevalences of 31–45% in tomato plots in Benin, with phylotyping confirming the dominance of phylotype I strains. Opoku *et al*. (2021) documented *S. rolfsii* incidences of 22–39% in market garden plots in Ghana. The genetic and phenotypic diversity of *Ralstonia solanacearum* strains from Côte d'Ivoire was assessed on a collection of 168 strains taken from Solanaceae in the southern plains and the western highlands with a dominance of phylotypes I, II (N'Guessan *et al*., 2012).

This study therefore aims to test the hypothesis of ecological niche partitioning between *S. rolfsii* and *R. solanacearum*, with direct implications for crop protection. The null hypothesis (H_0) posits a random co-occurrence of the two pathogens, independent of local edaphic conditions. The alternative hypothesis (H_1) predicts a spatial segregation determined by divergent ecological optima. The specific objectives are: (i) to map the prevalence and determine the statistical nature of their co-occurrence across five contrasting agroecological zones; and (ii) to identify the edaphic determinants driving their respective distribution. This work establishes a quantitative diagnosis necessary for the transition from uniform control to site-specific management strategies adapted to the heterogeneity of agroecosystems.

MATERIALS AND METHODS

Study Area and Sampling Design

A cross-sectional epidemiological survey was conducted from February to August 2024, covering a latitudinal gradient representative of the pedoclimatic diversity of Côte d'Ivoire. The study targeted five distinct agroecological zones (AEZ; Figure 1), extending from the humid sub-equatorial climate (AEZ I, Abidjan) to the semi-arid Sudanian savannas (AEZ VI, Korhogo). A stratified random sampling design was applied. Within each AEZ, 30 tomato (*S. lycopersicum*) agroecosystems were selected (total $n = 150$), ensuring a statistical power ($1-\beta$) of 0.80 for the detection of medium-sized effects ($w = 0.3$; $\alpha = 0.05$), calculated a priori according to the method of Cohen (1988). The inclusion criteria for plots were: (i) an active fruiting phenological stage (45–90 days after transplanting), and (ii) the absence of biocidal treatments during the 21 days preceding the survey.

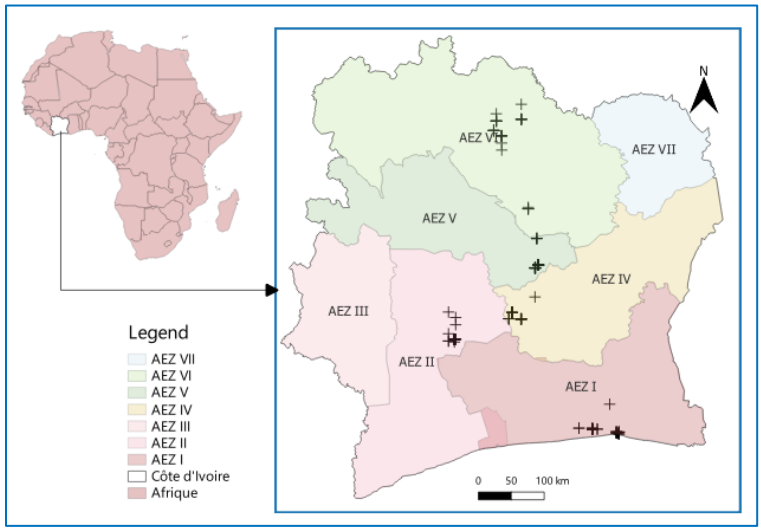

The map illustrates the latitudinal gradient studied, from the humid coastal zone (AEZ I, Abidjan) to the Sudanian savanna (AEZ VI, Korhogo). Each symbol (+) represents a survey zone. The decreasing rainfall gradient (2,400 to 1,000 mm/year) is indicated by the arrow.

Figure 1. Geographic location of the 150 tomato agroecosystems sampled across the five agroecological zones (AEZ) of Côte d'Ivoire.

Disease Assessment and Pathogen Identification

In each plot, disease incidence and severity were assessed on a cohort of 30 plants sampled along a diagonal transect. Incidence was calculated as the percentage of plants exhibiting characteristic symptoms. Severity was rated on an ordinal scale from 0 to 4 (Table 1), adapted from Punja (1985) for *S. rolfsii* and from Hayward (1991) for *R. solanacearum*. The Disease Severity Index (DSI) was calculated for each plot according to the McKinney (1923) equation:

$$DSI = [\Sigma (n_i \times v_i) / (N \times V)] \times 100$$

where: n_i is the number of plants in severity class i; v_i is the numerical value of class i (0 to 4); N is the total number of plants assessed (N = 30); and V is the maximum scale value (V = 4). Error bars in figures represent the standard error of the mean (SEM).

Table 1. Ordinal severity scale (0–4) used for symptom assessment of southern blight and bacterial wilt.

Rating	Symptom Description
0	Healthy plant, no symptoms
1	Mild symptoms: lesion limited to the collar (*S. rolfsii*) or wilting of a single leaf (*R. solanacearum*)
2	Moderate symptoms: visible mycelium on 50% of the collar (*S. rolfsii*) or wilting of 2–3 leaves (*R. solanacearum*)
3	Severe symptoms: extensive necrosis with sclerotia (*S. rolfsii*) or generalized wilting (*R. solanacearum*)
4	Dead or completely wilted plant

Ordinal severity scale (0–4) used for symptom assessment of southern blight (S. rolfsii) and bacterial wilt (R. solanacearum). Adapted from Punja (1985) and Hayward (1991).

Pathogen diagnosis combined *in situ* symptomatology and *ex situ* microbiological identification. For *S. rolfsii*, confirmation was achieved by isolation on Potato Dextrose Agar (PDA) amended with chloramphenicol (250 mg/L). For *R. solanacearum*, the bacterial etiology was confirmed by isolation on Kelman medium (Kelman, 1954) modified with 2,3,5-triphenyltetrazolium chloride (TZC, final concentration 50 mg/L). Inter-rater reliability was validated by an Intraclass Correlation Coefficient (ICC) test, yielding an ICC of 0.89 (95% CI [0.82–0.94]) (Koo & Li, 2016).

Soil Physicochemical Characterisation

For each site, a composite soil sample was constituted from five cores collected according to an X-pattern within the 0–20 cm horizon at the same time as the epidemiological survey. Samples were collected on the same day as the plant disease assessment, within a 30 cm radius of the collar of the scored plant. Approximately 500 g per plot were collected and immediately sealed in airtight bags and transported to the laboratory. Upon receipt, samples were air-dried at 25°C for 48 hours, then sieved at 2 mm to remove plant debris and stones prior to analysis. Physicochemical analyses were performed according to standardised protocols: soil pH (ISO 10390, soil:water ratio 1:2.5), total organic carbon (TOC, Walkley-Black method), total nitrogen (TN, Kjeldahl method), and cation exchange capacity (CEC, ammonium acetate method at pH 7). Analytical quality was controlled with a coefficient of variation (CV) below 5%.

Statistical Analyses

All statistical analyses were performed using R (Version 4.4.1) (R Core Team, 2024). Due to the non-Gaussian distribution of epidemiological data, non-parametric tests were systematically employed (Madden *et al.,* 2007). Variations in prevalence and DSI among the five AEZ were tested by the Kruskal-Wallis test, followed by Dunn's multiple comparison post-hoc test with Benjamini-Hochberg correction (FDR < 0.05). The hypothesis of independence was tested by calculating the Odds Ratio (OR) and a Chi-square (χ^2) test. Relationships between DSI and edaphic variables were quantified by the Spearman rank correlation coefficient (ρ), an approach appropriate for non-Gaussian data that detects monotonic associations. This choice was further justified by the sample size available per zone (n = 30), which is insufficient to reliably estimate the smoothing functions of Generalised Additive Models (GAM) without risk of overfitting, as these models generally require a minimum of 10 to 15 observations per effective degree of freedom of the smoothing terms (Wood, 2017). The significance threshold was set at $\alpha = 0.05$.

RESULTS

Structure of the Pathogen Community: Statistical Independence

The phytosanitary survey reveals a predominance of mono-infections. Across the entire gradient, 52.0% of plots (n = 78) exhibited symptoms of at least one

soilborne disease. *Sclerotium rolfsii* was the most frequently detected pathogen, occurring as a single infection in 30.0% of plots (n = 45), followed by *Ralstonia solanacearum* with 12.7% (n = 19) (Figure 2).

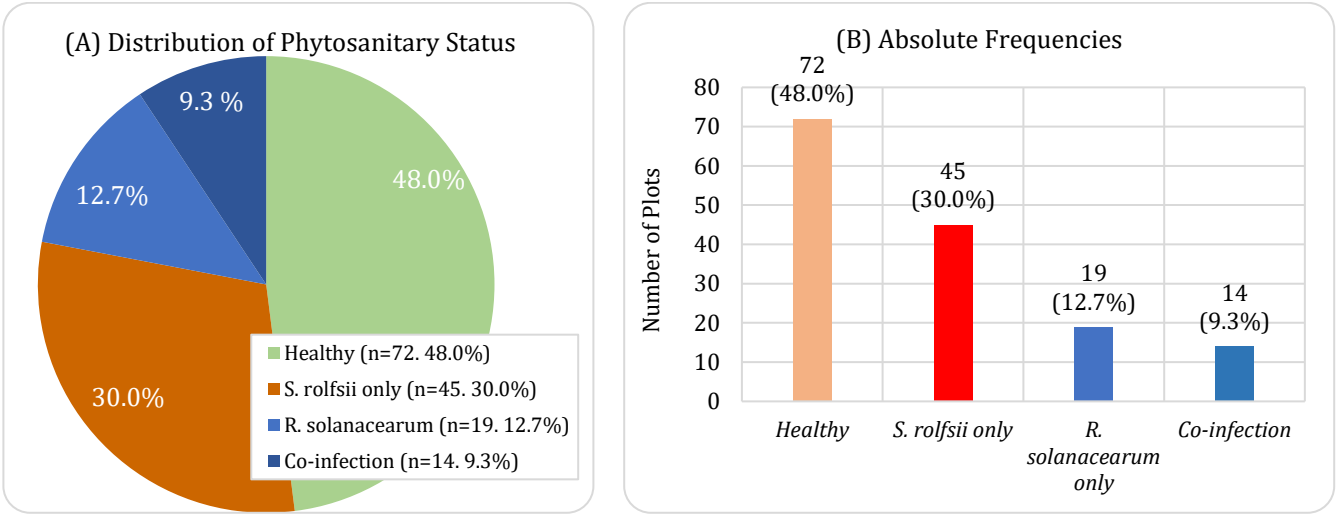

Figure 2. Structure of the soilborne pathological complex: relative prevalence of mono-infections and co-infections. *Diagram illustrating the distribution of phytosanitary status across the 150 tomato plots. Healthy: absence of symptoms (48.0%). Southern blight only: exclusive infection by S. rolfsii (30.0%). Bacterial wilt only: exclusive infection by R. solanacearum (12.7%). Co-infection: simultaneous presence of both pathogens (9.3%). The low proportion of co-infections and the non-significant Odds Ratio (OR = 1.18; p = 0.834) confirm the spatial independence of the two pathogens.*

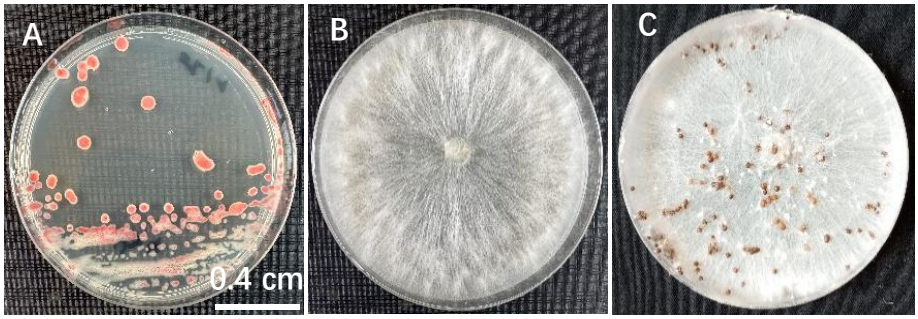

Figure 3. Morphological and cultural characteristics used for pathogen identification.
(A) Virulent colonies of R. solanacearum on modified Kelman agar (TZC) exhibiting irregular fluidity and a characteristic red center. (B) Silky white mycelium of S. rolfsii on PDA agar at 5 days. (C) Formation of mature spherical sclerotia (survival structures) on PDA agar at 21 days.

Co-infection situations were marginal, representing only 9.3% of plots (n = 14) (Table 2). The co-occurrence analysis confirms strict statistical independence between the two pathogens (χ^2 = 0.044; df = 1; p = 0.834). The Odds Ratio of 1.18 (95% CI [0.54–2.58]) indicates the absence of any significant synergistic or antagonistic association.

Table 2. Contingency table of the co-occurrence of *S. rolfsii* and *R. solanacearum* across the 150 tomato plots in Côte d'Ivoire.

	R. solanacearum (+)	*R. solanacearum* (−)	Total
S. rolfsii (+)	14 (9.3%)	45 (30.0%)	59 (39.3%)
S. rolfsii (−)	19 (12.7%)	72 (48.0%)	91 (60.7%)
Total	33 (22.0%)	117 (78.0%)	150 (100%)

Chi-square test: χ^2 = 0.044; df = 1; p = 0.834. Odds Ratio = 1.18 (95% CI [0.54–2.58]). The absence of statistical significance confirms the independence between the two pathogens. Values in parentheses represent percentages relative to the total (N = 150). +: pathogen presence; −: pathogen absence.

Spatial Segregation along the Latitudinal Gradient

The distribution of pathogens was not uniform but strongly structured by the agroecological zone. Bacterial wilt (*R. solanacearum*) exhibited a tropical humid specialist profile, forming an endemic hotspot in the coastal zone (Abidjan), where it saturated 76.7% of plots (Table 3) with maximum severity (DSI = 19.9 ± 1.4). Its epidemiological pressure decreased abruptly northward (Kruskal-Wallis: H = 75.99; df = 4; $p < 0.001$). Southern blight (*S. rolfsii*) expressed a more ubiquitous strategy but with an inverse climatic optimum, maximising its fitness in the northern savannas (Korhogo, prevalence = 63.3%; Table 3; DSI = 13.2 ± 1.1) (Kruskal-Wallis: H = 16.09; df = 4; $p = 0.003$; Table 3).

Table 3. Spatial variation in epidemiological intensity of the *S. rolfsii*–*R. solanacearum* complex along the agroecological gradient in Côte d'Ivoire (N = 150).

Agroecological Zone	Climate	n	Prevalence *S. rolfsii* (%)	DSI *S. rolfsii* (Mean ± SE)	Prevalence *R. solanacearum* (%)	DSI *R. solanacearum* (Mean ± SE)
Abidjan	Humid Coastal	30	43.3	10.2 ± 1.2 ^{ab}	76.7	19.9 ± 1.4 ^{a}
Yamoussoukro	Guinean Savanna	30	46.7	13.0 ± 1.3 ^{a}	26.7	5.1 ± 0.8 ^{b}
Korhogo	Sudanian Savanna	30	63.3	13.2 ± 1.1 ^{a}	0.0	0.0 ± 0.0 ^{c}
Daloa	Transitional Forest	30	26.7	8.2 ± 0.9 ^{ab}	0.0	0.0 ± 0.0 ^{c}
Bouaké	Transition	30	16.7	1.7 ± 0.3 ^{b}	6.7	0.4 ± 0.1 ^{c}
Test (Kruskal-Wallis)				H = 16.09; p = 0.003		H = 75.99; p < 0.001

Values represent the mean ± standard error (SE). DSI: Disease Severity Index (0–100), calculated according to the McKinney equation with a severity scale of 0 to 4. Superscript letters (^{a}, ^{b}, ^{c}) indicate significant differences between zones for the same pathogen (Dunn's post-hoc test with Benjamini-Hochberg correction, FDR < 0.05). n = number of plots per zone.

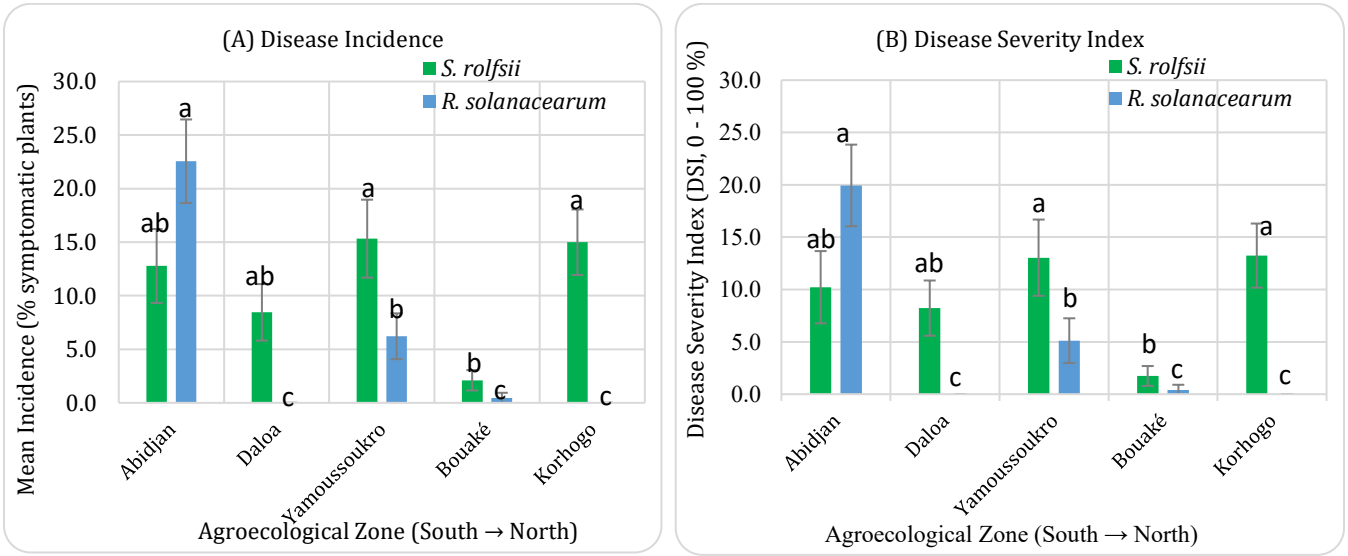

Figure 4. Comparative incidence and severity of *Sclerotium rolfsii* and *Ralstonia solanacearum* along the bioclimatic gradient.

Histograms represent the mean incidence (% symptomatic plants) ± standard error (SEM, n = 30 per zone). Distinct letters above bars indicate statistically significant differences according to the Kruskal-Wallis test followed by Dunn's post-hoc test (FDR < 0.05). The graph highlights the spatial segregation between bacterial wilt (dominant in the south, Abidjan) and southern blight (dominant in the savannas, Korhogo/Yamoussoukro). Zones are ordered from south (left) to north (right) along the latitudinal gradient.

Edaphic Drivers and Niche Partitioning

Soil analysis revealed significant variability in edaphic parameters across the different agroecological zones. The Yamoussoukro zone stood out with the highest values for all parameters: water pH (6.91), organic carbon (2.73%), organic matter (4.69%), total nitrogen (0.22%), and CEC (25.65 $cmol^+/kg$). In contrast, Korhogo presented the lowest values for organic carbon (1.33%), organic matter (2.28%), and total nitrogen (0.11%), but showed a relatively high CEC (19.74 $cmol^+/kg$). The Abidjan, Bouaké, and Daloa zones displayed intermediate and relatively homogeneous values for most parameters (Table 4).

The Spearman correlation analysis reveals a clear divergence in the ecological preferences of the two pathogens (Table 5). The intensity of bacterial wilt was inversely correlated with soil pH ($\rho = -0.28$; $p < 0.001$) and Cation Exchange Capacity ($\rho = -0.35$; $p < 0.001$). Conversely, *S. rolfsii* showed a significant positive affinity for organic matter ($\rho = +0.23$; $p < 0.01$) and total organic carbon ($\rho = +0.21$; $p < 0.01$).

Table 4. Soil edaphic properties across the five agroecological zones of Côte d'Ivoire.

Agroecological zones	Mean ± Standard Error				
	pH water	Total organic carbon (%)	Organic matter (%)	Total nitrogen (%)	CEC ($cmol^+/kg$)
Abidjan	6.12 ± 0.30 cd	1.68 ± 0.32 ab	2.89 ± 0.55 b	0.16 ± 0.01 b	14.59 ± 3.69 c
Bouaké	6.47 ± 0.17 bc	1.80 ± 0.69 ab	3.10 ± 1.19 b	0.15 ± 0.04 b	13.30 ± 3.91 c
Daloa	6.11 ± 0.47 d	1.92 ± 0.40 b	3.30 ± 0.69 ab	0.17 ± 0.02 b	14.89 ± 5.28 c
Korhogo	6.57 ± 0.58 ab	1.33 ± 0.04 c	2.28 ± 0.07 b	0.11 ± 0.01 c	19.74 ± 1.36 b
Yamoussoukro	6.91 ± 0.24 a	2.73 ± 0.05 a	4.69 ± 0.09 a	0.22 ± 0.00 a	25.65 ± 2.15 a
Kruskal-Wallis p-value	0.0000	0.0000	0.0000	0.0000	0.0000

Superscript letters (a, b, c, d) within each column indicate homogeneous groups determined by Dunn's post-hoc test after Kruskal-Wallis ($p < 0.05$). Zones sharing the same letter are not statistically different. CEC ($cmol^+/kg$) = Cation Exchange Capacity ($cmol^+/kg$)

Table 5. Spearman correlation matrix (ρ) between soil physicochemical parameters and disease intensity (DSI) across the 150 plots.

Edaphic Parameter	DSI *S. rolfsii* (ρ)	DSI *R. solanacearum* (ρ)
Water pH	+0.05 ^{ns}	−0.28 ***
Total Organic Carbon (%)	+0.21 **	−0.09 ^{ns}
Organic Matter (%)	+0.23 **	−0.11 ^{ns}
Total Nitrogen (%)	+0.18 *	−0.06 ^{ns}
CEC ($cmol^+/kg$)	+0.08 ^{ns}	−0.35 ***

*ρ = Spearman rank correlation coefficient. Significance levels: * $p < 0.05$; ** $p < 0.01$; *** $p < 0.001$; ^{ns} = non-significant. Bold values indicate significant correlations. The divergence of signs (positive for S. rolfsii, negative for R. solanacearum) confirms the existence of opposing ecological optima, characteristic of edaphic niche partitioning.*

Moderating Factors: Topography and Weed Management

Uncontrolled weed growth constituted a universal risk factor, significantly increasing the DSI for both pathogens ($p < 0.05$). Hydromorphic lowlands drastically amplified bacterial wilt severity (DSI multiplied by 3 compared to uplands; $p < 0.001$), while *S. rolfsii* better tolerated drained upslope positions (Figure 5).

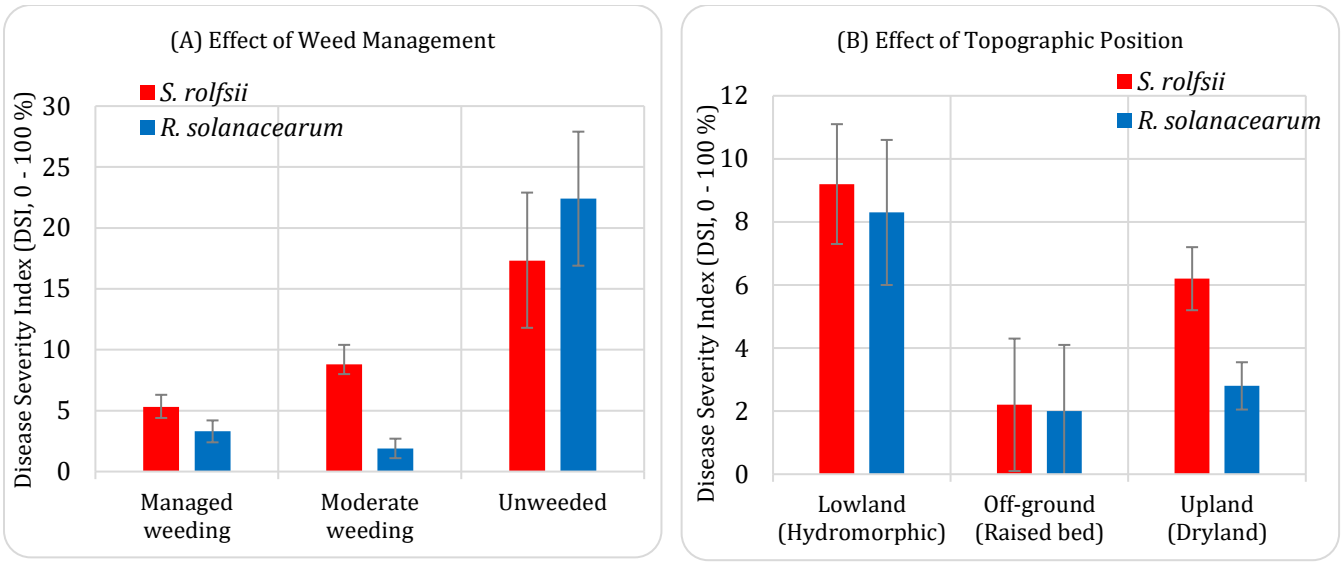

Figure 5. Influence of cultural practices and topography on soilborne disease expression.

(A) Impact of weed management on the Disease Severity Index (DSI). (B) Effect of plot topographic position on DSI. Error bars represent the standard error (SEM). Distinct letters indicate significant differences (Mann-Whitney test, $p < 0.05$). Hydromorphic lowlands constitute a major and specific risk factor for R. solanacearum (DSI × 3), while uncontrolled weed growth is a universal risk factor for both pathogens.

DISCUSSION

This study challenges the classical phytopathological paradigm of the disease complex, which frequently presupposes a facilitative synergy between sympatric soilborne pathogens. Conversely, our results demonstrate a statistically independent coexistence (OR = 1.18; $p = 0.834$) between *S. rolfsii* and *R. solanacearum*. This absence of synergy suggests that the assembly of this pathobiome is associated not with trophic cooperation, but with a process consistent with environmental filtering. This observation is in agreement with, in a tropical West African context, the ecological niche theory for pathogens (Fodor, 2011) and the microbial ecology models of Bass *et al.* (2019) and Delgado-Baquerizo *et al.* (2020), stipulating that abiotic niche partitioning constitutes the dominant mechanism of species segregation in heterogeneous soils.

The negative correlation between bacterial wilt and soil pH ($\rho = -0.28$) aligns with recent physiological discoveries demonstrating differential root colonization patterns in *R. solanacearum* (Caldwell *et al*., 2017). We hypothesise that soil acidity may indirectly favour *R. solanacearum* by potentially inhibiting antagonistic microflora, thereby reducing the immune resistance of the soil (Liu *et al.,* 2023; Zhang *et al.,* 2022). In contrast, *S. rolfsii* adopts a saprobic competitor strategy. Its positive correlation with organic matter content ($\rho = +0.23$) explains its persistence in savanna zones. Its sclerotia, extremely resistant survival structures, can persist in the soil for several years (Punja, 1985). In savanna zones, cycles of burning and decomposition of crop residues enrich the superficial horizons with organic carbon, creating a favourable substrate for sclerotial germination and mycelial growth.

The observed patterns of niche partitioning suggest that the one-size-fits-all approach often applied in tropical crop protection may be inadequate. Sustainable management could therefore benefit from spatially differentiated, site-specific strategies based on local edaphic diagnosis.

The observed soil associations have direct implications for disease management adapted to the specific characteristics of small farms. In coastal areas where relatively acidic soil conditions are associated with bacterial wilt (AEZ I, Abidjan), the priority intervention should be the use of acid-tolerant tomato varieties (Lebeau *et al*., 2011) and the application of mature compost or biochar to improve soil biological resistance (Irfan & Mirara, 2024). In northern savanna areas where the incidence of S. rolfsii is highest (AEZ VI, Korhogo), recommended practices should include reduced planting density (60 cm × 80 cm spacing) to limit the spread of

mycelium between plants (Rivard *et al*., 2010), the application of plastic mulch or rice straw as a physical barrier against sclerotia contact with stems (Punja, 1985), and the inclusion of non-host crops such as cowpea or maize in crop rotation sequences to reduce sclerotial inoculum density over time (Sneh *et al*., 1996). For all zones, weed management remains an essential prophylactic measure, as weeds act as epidemiological bridges that transcend specific edaphic niches (Agrios, 2005).

This study presents several limitations. First, the cross-sectional design (February–August 2024) aggregates samples collected in dry and wet seasons into a single static pool. This approach does not allow causal inference nor capture temporal dynamics, and it ignores seasonal variations in soil moisture, which directly influence flagellar motility of R. solanacearum (Genin, 2010) and sclerotia germination of *S. rolfsii* (Punja, 1985), thus introducing potential bias in the interpretation of edaphic associations. The spatial associations documented here are consistent with environmental filtering but cannot exclude two alternative community assembly mechanisms: competitive exclusion and historical contingency (Kraft *et al*., 2015). Second, pathogen identification relies exclusively on morphological and cultural criteria, without molecular confirmation, whereas the *R. solanacearum* species complex requires phylotyping for accurate characterization (Prior *et al*., 2016). Third, the absence of soil microbiome data limits the understanding of underlying suppressiveness mechanisms, rendering our hypotheses on this topic speculative (Schlatter *et al.,* 2017). Fourth, tomato variety diversity across zones (locally tolerant vs. improved susceptible varieties) represents a potential confounding factor that may independently influence incidence patterns (Lebeau *et al.,* 2011). These limitations constitute hypotheses whose verification, coupled with validation trials in a controlled environment, would allow us to test the proposed differentiated management strategies. Contrary to the cross-sectional design of this study, these longitudinal and experimental approaches could establish causal links.

CONCLUSION

This study provides the first quantitative evidence suggesting that the structure of the tomato soilborne pathogen community in Côte d'Ivoire co-varies with niche partitioning patterns rather than with synergistic interactions. Environmental filtering appears as a plausible driver of their distribution: edaphic acidity is associated with *R. solanacearum* in coastal zones, while organic carbon availability is associated with higher prevalence of *S. rolfsii* in the savannas. These associations suggest a paradigm shift for tropical crop protection: moving away from uniform control strategies towards precision epidemiology based on physicochemical risk mapping.

ACKNOWLEDGEMENT:

Authors are thankful to the tomato growers for their valuable help.

FUNDING ACKNOWLEDGEMENT STATEMENT

Supported by the Centre of Excellence for Climate Change, Biodiversity and Sustainable Agriculture.

CONFLICT OF INTEREST

The authors declare that they have no known conflict of interest that could have appeared to influence the work reported in this paper.

REFERENCES

Agrios, G. N. 2005. Plant diseases caused by fungi, Plant Pathology, 5th ed. Elsevier, Amsterdam, Netherlands. p. 385-614.

Bass, D., G. D. Stentiford, H. C. Wang, B. Koskella and C. R. Tyler. 2019. The pathobiome in animal and plant diseases. *Trends in Ecology & Evolution*, 34: 996-1008.

Bolou, B. B. A., A. Kouabenan, M. Doumbouya, G. Kouamé, F. Kassi, S. Tuo, N. Koné, P. Kouassi and K. Daouda. 2016. Analysis of sclerotinia expression due to *Sclerotium rolfsii* fungus in market gardening crops in the different agroecological zones of Côte d'Ivoire. *Journal of Agriculture and Ecology Research International*, 6: 1-12.

Caldwell, D., B. S. Kim and A. S. Iyer-Pascuzzi. 2017. *Ralstonia solanacearum* differentially colonizes roots of resistant and susceptible tomato plants. *Phytopathology*, 107: 528-536.

Cohen, J. 1988. Statistical Power Analysis for the Behavioral Sciences. 2nd ed. Lawrence Erlbaum Associates, Hillsdale.

Delgado-Baquerizo, M., C. A. Guerra, C. Cano-Díaz, E. Egidi,

J. Wang and N. Eisenhauer. 2020. The proportion of soil-borne pathogens increases with warming at the global scale. *Nature Climate Change*, 10: 550-554.

Dossoumou, M. E., R. Sikirou, A. Zannou, M. Paret and L. Baba-Moussa. 2023. Bacterial wilt and dissemination factors in tomato production areas of Benin, West Africa. *Archives of Phytopathology and Plant Protection*, 56: 1427-1449.

Fodor, E. 2011. Ecological niche of plant pathogens. *Annals of Forest Research*, 54: 3-21.

Genin, S. 2010. Molecular traits controlling host range and adaptation to plants in *Ralstonia solanacearum*. *New Phytologist*, 187: 920-928.

Hayward, A. C. 1991. Biology and epidemiology of bacterial wilt caused by *Pseudomonas solanacearum*. *Annual Review of Phytopathology*, 29: 65-87.

Irfan, M. F. and F. Mirara. 2024. Biochar application in improving soil health and sustainability. *Bulletin of Biological and Allied Sciences Research*, 9: 81.

Kelman, A. 1954. The relationship of pathogenicity in *Pseudomonas solanacearum* to colony appearance on a tetrazolium medium. *Phytopathology*, 44: 693-695.

Koo, T. K. and M. Y. Li. 2016. A guideline of selecting and reporting intraclass correlation coefficients for reliability research. *Journal of Chiropractic Medicine*, 15: 155-163.

Kraft, N. J. B., P. B. Adler, O. Godoy, E. C. James, S. Fuller and J. M. Levine. 2015. Community assembly, coexistence and the environmental filtering metaphor. *Functional Ecology*, 29: 592-599.

Lamichhane, J. R. and V. Venturi. 2015. Synergisms between microbial pathogens in plant disease complexes: A growing trend. *Frontiers in Plant Science*, 6: 385.

Lebeau, A., M. C. Daunay, A. Frary, A. Palloix, J. F. Wang, J. Dintinger, F. Chiroleu, E. Wicker and P. Prior. 2011. Bacterial wilt resistance in tomato, pepper, and eggplant: genetic resources respond to diverse strains in the *Ralstonia solanacearum* species complex. Phytopathology, 101: 154-165.

Liu, L., Z. Chen, Z. Su, S. Li, A. Ali, Z. Cai and X. Huang. 2023. Soil pH indirectly determines *Ralstonia solanacearum* colonization through its impacts on microbial networks and specific microbial groups. *Plant and Soil*, 482: 73-88.

Madden, L. V., G. Hughes and F. van den Bosch. 2007. The Study of Plant Disease Epidemics. APS Press, St. Paul.s

McKinney, H. H. 1923. Influence of soil temperature and moisture on infection of wheat seedlings by *Helminthosporium sativum*. *Journal of Agricultural Research*, 26: 195-217.

N'Guessan, C. A., K. Abo, L. Fondio, F. Chiroleu, A. Lebeau, S. Poussier, E. Wicker and D. Koné. 2012. So near and yet so far: The specific case of *Ralstonia solanacearum* populations from Côte d'Ivoire in Africa. *Phytopathology*, 102: 733-740.

Opoku, B. A., C. Kwoseh, E. Gyasi and E. Moses. 2021. Incidence and severity of major fungal diseases on tomato in three districts within the forest and forest-savannah agro-ecological zones of Ghana. *Ghana Journal of Agricultural Science*, 56: 46-60.

Prior, P., F. Ailloud, B. L. Dalsing, B. Remenant, B. Sanchez and C. Allen. 2016. Genomic and proteomic evidence supporting the division of the *Ralstonia solanacearum* species complex into three species. *BMC Genomics*, 17: 90.

Punja, Z. K. 1985. The biology, ecology, and control of *Sclerotium rolfsii*. *Annual Review of Phytopathology*, 23: 97-127.

R Core Team. 2024. R: A Language and Environment for Statistical Computing. R Foundation for Statistical Computing, Vienna.

Rivard, C. L., S. O'Connell, M. M. Peet and F. J. Louws. 2010. Grafting tomato with interspecific rootstock to manage diseases caused by *Sclerotium rolfsii* and southern root-knot nematode. *Plant Disease*, 94: 1015-1021.

Schlatter, D. C., L. Kinkel, L. S. Thomashow, D. M. Weller and T. C. Paulitz. 2017. Disease suppressive soils: new insights from the soil microbiome. *Phytopathology*, 107: 1284-1297.

Sneh, B. 1996. Rhizoctonia Species: taxonomy, molecular biology, ecology, pathology and disease control. Springer, Berlin, Germany.

Wang, Z., W. Luo, S. Cheng, H. Zhang, J. Zong and Z. Zhang. 2023. *Ralstonia solanacearum* – A soil borne hidden enemy of plants: Research development in management strategies, their action mechanism and challenges. *Frontiers in Plant Science*, 14: 1141902.

Wei, Z., Y. Gu, V. P. Friman, G. A. Kowalchuk, Y. Xu, Q. Shen and A. Jousset. 2019. Initial soil microbiome composition and functioning predetermine future plant health. *Science Advances*, 5: eaaw0759.

Wood, S. N. 2017. Generalized Additive Models: An Introduction with R. 2nd ed. CRC Press/Taylor & Francis Group, Boca Raton.

Zhang, S., X. Liu, L. Zhou, L. Deng, W. Zhao, Y. Liu and W. Ding. 2022. Alleviating soil acidification could increase disease suppression of bacterial wilt by recruiting potentially beneficial rhizobacteria. *Microbiology Spectrum*, 10: e02333-21.